NASA Technical Memorandum 106745

Centrifugal and Axial Pump Design and Off-Design Performance Prediction

Joseph P. Veres
Lewis Research Center
Cleveland, Ohio

National Aeronautics and
Space Administration

CENTRIFUGAL AND AXIAL PUMP DESIGN AND OFF-DESIGN PERFORMANCE PREDICTION

Joseph P. Veres
National Aeronautics and Space Administration
Lewis Research Center
Cleveland, Ohio 44135

SUMMARY

A meanline pump-flow modeling method has been developed to provide a fast capability for modeling pumps of cryogenic rocket engines. Based on this method, a meanline pump-flow code PUMPA was written that can predict the performance of pumps at off-design operating conditions, given the loss of the diffusion system at the design point. The design-point rotor efficiency and slip factor are obtained from empirical correlations to rotor-specific speed and geometry. The pump code can model axial, inducer, mixed-flow, and centrifugal pumps and can model multistage pumps in series. The rapid input setup and computer run time for this meanline pump flow code make it an effective analysis and conceptual design tool. The map-generation capabilities of the code provide the information needed for interfacing with a rocket engine system modeling code. The off-design and multistage modeling capabilities of PUMPA permit the user to do parametric design space exploration of candidate pump configurations and to provide head-flow maps for engine system evaluation.

INTRODUCTION

During the conceptual design phase of new liquid-propellant rocket engine systems, the performance of the turbopumps at off-design operating conditions can influence the design of the pump. A high degree of engine throttling can be a design requirement for launch vehicle upper stages, orbit transfer vehicles (OTV), and landers (ref. 1). In the design process of pumps, a single operating point used to optimize the geometry may not be adequate because of often conflicting system requirements. With knowledge of the flow physics at off-design conditions, the designer can optimize the pump configuration to provide acceptable pump and system performance during engine throttling. The ability to predict pump off-design performance is necessary for system evaluation of turbopumps within rocket engines. A meanline flow modeling code for pumps, PUMPA, was written to provide a rapid evaluation of candidate pump design concepts. The PUMPA code also predicts pump performance at all operating conditions encountered during engine and turbopump throttling.

PUMPA is based on the Euler equation (eq. (11)) coupled with empirical correlations for rotor efficiency. Once the design operating performance is established, the code can estimate the off-design characteristic performance map. The diffusion system loss at the design point is input and varied at off-design by an empirical relation. The match between the pump rotor and the diffusion system influences the slope of the pump map and can effect the location of the stall and cavitation inception lines. The suction performance at off-design conditions is based on empirical correlations to the suction performance at design. The flow where the static pressure at the tip is equal to the vapor pressure determines the cavitation inception point. The pump stall criteria is an empirically derived correlation to the static pressure recovery coefficient of the vaneless diffuser. The pump configuration, flowpath, and number of stages that will result in an acceptable system performance can be quickly determined by the use of this multistage meanline flow modeling method. This report contains a description of the capabilities of the PUMPA code and the equations with the definition of the variables. Included are validation cases from cryogenic rocket engine pumps and research pumps that have been flow-modeled with the PUMPA computer code.

CAPABILITIES OF PUMP MEANLINE FLOW CODE: PUMPA

The pump meanline flow modeling method can be used to model the following pump configurations: axial, inducer, mixed-flow, and centrifugal. The PUMPA flow code has multistage capability with up to four stages in series. The code provides an estimate of flow incidences, losses, and cavitation inception at off-design operating conditions. Both the rotor efficiency and the slip factor can be modified to match test data by means of correction factors which otherwise have a default value of 1.0.

PUMPA can estimate pump performance at off-design operating conditions using the default values of rotor efficiency, slip factor, and diffusion system loss at the design point. For a given set of pump inlet pressure and temperature, the PUMPA code can generate a performance characteristic map. Fluid options are liquid hydrogen, liquid oxygen, liquid nitrogen, JP–4, water, and air. Fluid properties are obtained from GASPLUS (ref. 2) except JP–4.

INPUT TO MEANLINE FLOW MODEL

To create a meanline flow model of a pump with the PUMPA code, a minimal number of dimensions are required to adequately describe the rotor and the diffusion system for each stage. Figure 1 shows the locations of some of the key parameters required to specify the dimensions of the rotor and the diffuser. The flowpath radii, span, and blade angles are input at the leading and trailing edges at both the hub and tip. The diffusion system dimensions are specified in terms of vaneless section inlet and exit radii, spans, volute or diffuser throat area, volute tongue or vaned diffuser leading edge angle, and stage exit area. Pump inlet fluid conditions are specified in terms of design rotational speed, fluid flow rate, pressure, temperature, and inlet swirl.
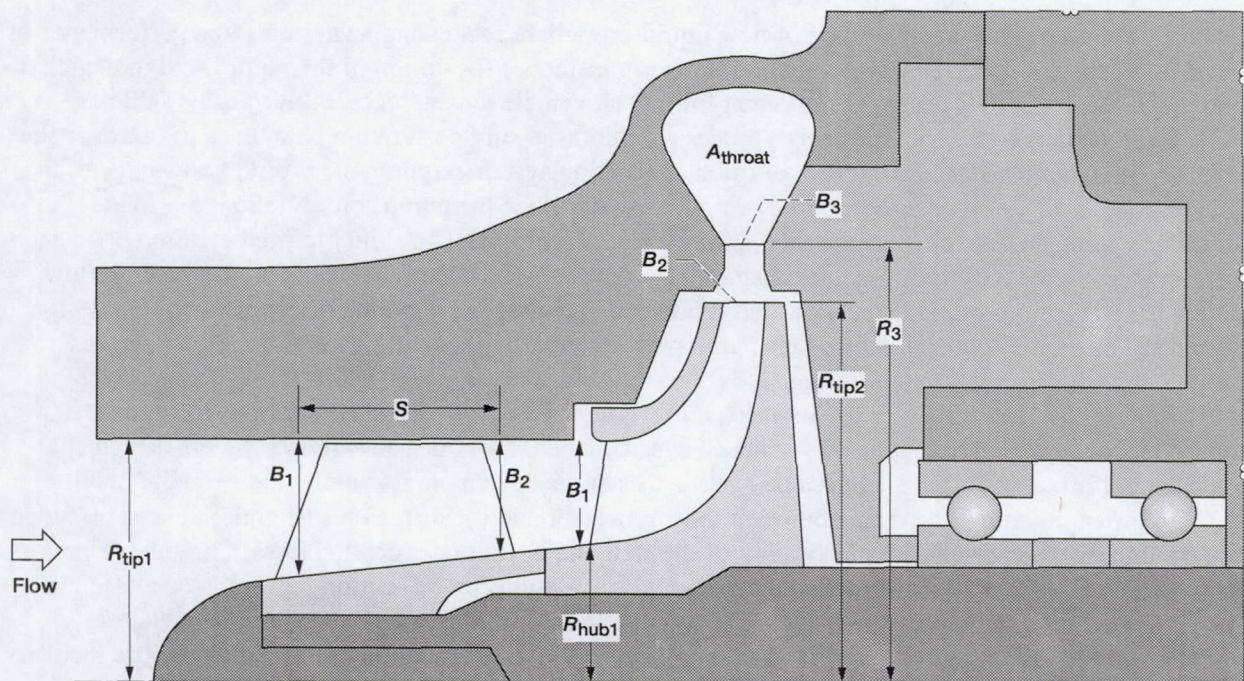

Figure 1.—Pump stage with axial inducer and centrifugal impeller.

OUTPUT OF MEANLINE FLOW MODEL

The PUMPA code output consists of flow conditions at the rotor leading and trailing edges, as well as the diffusion system inlet, throat, and outlet. In addition to the meanline flow conditions at the root-mean-square radius of the rotor, conditions at the hub and tip locations are also calculated. The output describes the flow conditions in terms of velocities, flow angles, pressures, and temperatures. Velocities and flow angles are calculated in both the relative and the absolute frames of reference. Static and total pressures and temperatures are calculated at the discharge of the rotor and stage. The total head rise, horsepower, and efficiency are summarized for each stage and for the overall pump. The calculation of all performance parameters is repeated at every point of an array of off-design conditions. The array of off-design conditions that is generated by the code consists of ten speed-lines, starting with the design speed, followed by incremental decreases of speed. The number of flow conditions to be analyzed per speed-line is specified in the input file. Three output files are generated by the code. The first (PUMPA.OUT) is quite large and contains a complete list of all of the calculated parameters within the pump at every point on the map. Post-processing of this output is required to determine the stall and cavitation inception lines. The two other output files that are created are condensed versions of the main output that contain summaries of the stage and overall performance and are used for plotting pump maps. Examples of several pump cross-sections and performance map plots are included in a subsequent section of this paper entitled "Examples of Pump Analyses."

THEORY AND EQUATIONS

Rotor Inlet Velocity Diagram

The flow area at the rotor inlet is calculated from the input flowpath dimensions by equation (1). The available flow area is compensated for the effects due to metal blockage of the rotor blade and the boundary layer blockage. The metal blockage is calculated by equation (2).

$$A_1 = \left[\pi B_1 \left(R_{\text{hub1}} + R_{\text{tip1}} \right) - Bk_1 \right] \lambda_1 \tag{1}$$

$$Bk_1 = \frac{Thk_1 \, B_1 \, Z_1}{\sin \beta_{B1}} \tag{2}$$

The blade blockage is included in the velocity triangle calculations in order to estimate the incidence angle just inside the blade after the flow impacts with the leading edge. When modeling rotors that have a large number of blades such as centrifugal impellers, it is particularly important to account for the effects of blade blockage. The meridional velocity of the fluid at the rotor leading edge root-mean-square diameter is:

$$C_{M1} = \frac{144 \, m}{\rho_1 A_1} \tag{3}$$

3

The blade tangential velocity is:

$$U = \frac{2\pi R N}{720} \tag{4}$$

Figure 2 shows the relevant constituents of a typical inlet velocity diagram.

Inlet flow with zero tangential velocity component is represented in figure 2 as having an absolute inlet flow angle of 90°. Flow that has positive prewhirl caused by prerotation with inlet guide vanes is represented by an inlet swirl angle that is less than 90°. The tangential component of velocity entering the rotor can be calculated in terms of the swirl angle of the flow as follows:

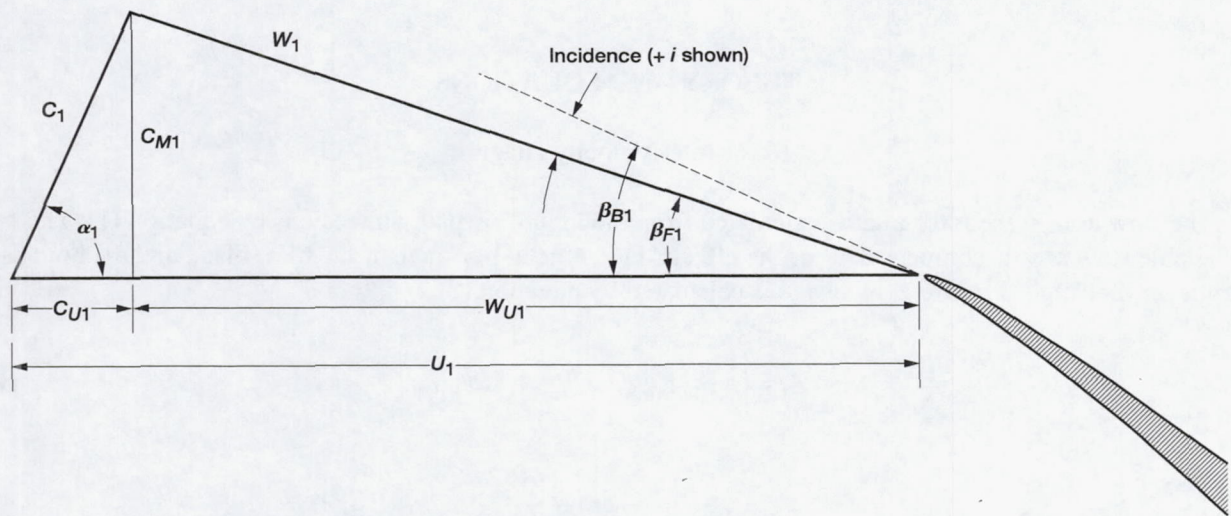$$C_{U1} = C_{M1} / \tan(\alpha_1) \tag{5}$$

Figure 2.—Rotor inlet velocity diagram.

The absolute fluid velocity at the rotor inlet, in terms of the meridional and the tangential components, is:

$$C_1 = \left(C_{M1}^{2} + C_{U1}^{2}\right)^{1/2} \tag{6}$$

The relative flow angle is:

$$\beta_{F1} = \tan^{-1} \frac{C_{M1}}{C_{U1} - U_1} \tag{7}$$

The incidence angle is the difference between the blade angle and the relative flow angle:

$$i_1 = \beta_{B1} - \beta_{F1} \tag{8}$$

4

The tangential component of the fluid's relative velocity is defined by

$$W_{U1} = C_{M1} \tan(90 - \beta_{F1}) \tag{9}$$

The meridional component of velocity in the absolute frame of reference is equal to the meridional component of velocity in the relative frame of reference. The relative fluid velocity is the vector sum of its tangential and meridional components as follows:

$$W_1 = \left(W_{U1}^2 + C_{M1}^2\right)^{1/2} \tag{10}$$

Rotor Head and Exit Velocity Diagram

The components of the rotor exit velocity diagram (refs. 3 and 4) are shown in the figure 3 velocity triangle, which shows the relationship between the absolute and relative velocities and flow angles.

The ideal head rise through the rotor is calculated from the Euler equation. The actual head rise is calculated iteratively in terms of the inlet and exit velocity triangles and the rotor hydraulic efficiency by the equation:

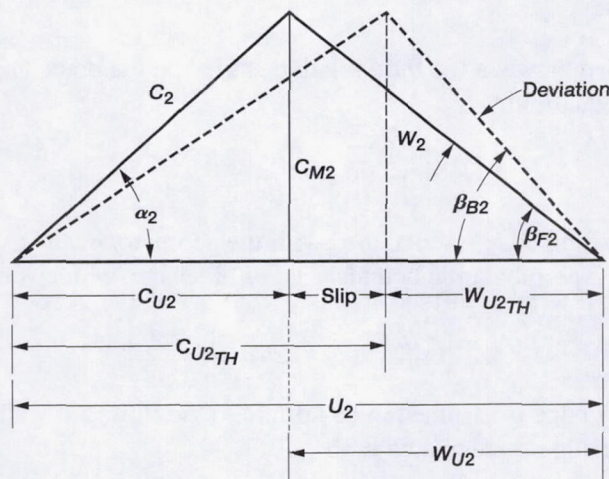$$H_2 = \left(U_2 \, C_{U2} - U_1 \, C_{U1}\right) \eta_{\text{hyd}} / g_c \tag{11}$$

Figure 3.—Rotor exit velocity diagram.

The rotor hydraulic efficiency is the ratio of actual head rise to the ideal head rise,

$$\eta_{\text{hyd}} = \frac{H_2}{H_{2i}} \tag{12}$$

The components of the velocity triangle are calculated at the hub, mean, and tip locations along the rotor blades. The meridional and tangential components of absolute velocity at the rotor trailing edge are calculated with equations (13) and (14), where the area is normal to the meridional component of velocity.

$$C_{M2} = \frac{144 \, m}{\rho_2 \, A_2} \tag{13}$$

5

$$C_{U2} = U_2 + W_{U2} \tag{14}$$

The tangential component of the fluid relative velocity is:

$$W_{U2} = C_{M2} \tan \beta_{B2} + U_2(1 - \sigma) \tag{15}$$

The slip is the difference between the theoretical and absolute fluid tangential velocities as described by the following equation:

$$\text{slip} = C_{U2_{TH}} - C_{U2} \tag{16}$$

The slip factor σ is:

$$\sigma = 1 - \frac{\text{slip}}{U_2} \tag{17}$$

The rotor exit relative flow angle is:

$$\beta_{F2} = \tan^{-1} \frac{C_{M2}}{W_{U2}} \tag{18}$$

The deviation is the difference between the fluid relative angle and the blade angle at the rotor exit as described by the following equation:

$$\text{deviation} = \beta_{B2} - \beta_{F2} \tag{19}$$

The flow area at the rotor trailing edge is calculated with the geometry of the exit flow area, including blade metal blockage, and the aerodynamic boundary layer blockage, which is estimated by using

$$A_2 = \left[\pi B_2 \left(R_{\text{tip2}} + R_{\text{hub2}} \right) - Bk_2 \right] \lambda_2 \tag{20}$$

The blade span at the trailing edge is assumed to be normal to the flowpath walls. The blade metal blockage at the rotor trailing edge is calculated with

$$Bk_2 = \frac{Thk_2 \, B_2 \, Z_2}{\sin \beta_{B2}} \tag{21}$$

The slip factor σ is also estimated by the PUMPA code, based on rotor geometry and empirical correlations. The slip factor that is predicted by the code for centrifugal impellers is based on the Pfleiderer correlation (ref. 5) and is calculated from the rotor geometry using equation (22). A default slip factor of 0.95 is used for inducers.

$$\frac{1}{\sigma} = 1 + \frac{1 + 0.6 \sin \beta_{B2}}{\left(Z_2 (1 + \delta) X^2 + 0.25 (1 - \delta)^2 \right)^{1/2}} \tag{22}$$

The PUMPA code has empirically derived rotor efficiency correlations based on tests of rocket engine turbopumps and compressor research rigs. The best efficiency point (BEP) for rotor hydraulic efficiency in terms of total-to-total conditions is determined from these correlations. The rotor BEP is at the design-point operating condition of flow and rotational speed. Figure 4 shows the BEP as a function of rotor dimensionless specific speed as used in the PUMPA code. The figure shows the relative location and expected efficiency levels for three basic types of pumps: (1) centrifugal, (2) mixed-flow, and (3) axial or inducer. The compressor polytropic efficiency derived in reference 6 is used as the hydraulic efficiency in PUMPA. Additional losses will be mentioned later. The dimensionless specific speed parameter shown in equation (23) is used to classify a wide range of rotor types, based on their kinematic and dynamic similarities.

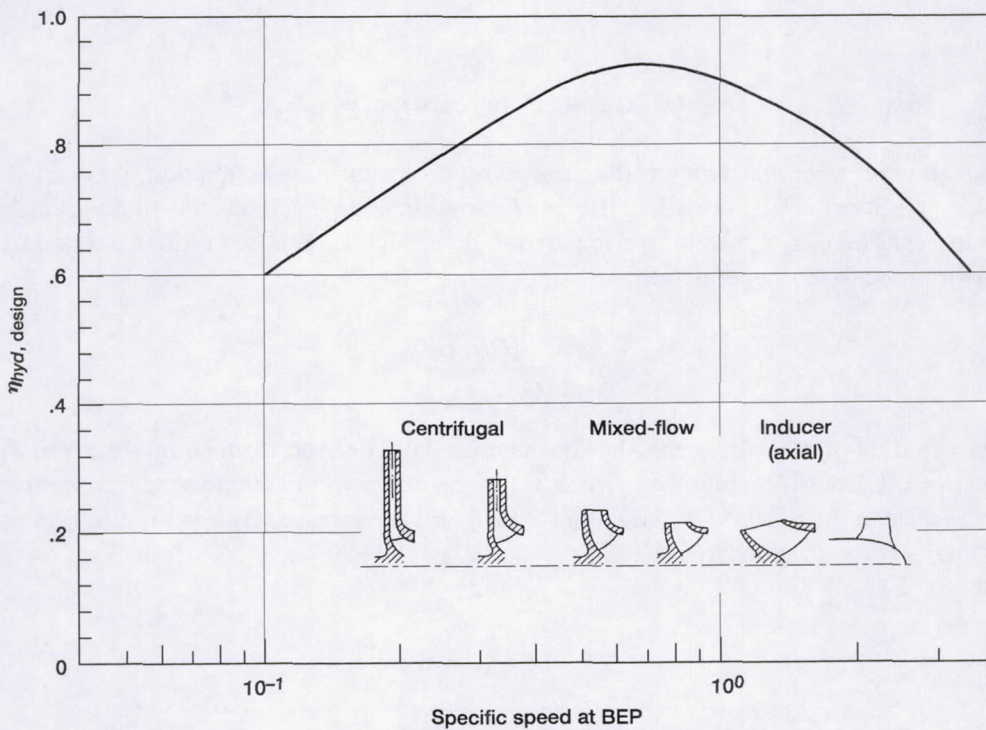$$Ns = \frac{\pi \, N \, Q^{1/2}}{30 \, g_c^{\,3/4} \, H_2^{\,3/4}} \tag{23}$$

Figure 4.—Rotor efficiency at BEP versus specific speed.

The following two polynomial equations show the variation of expected rotor efficiency levels for the range of pump configurations as a function of specific speed at the design point. Equation (24) applies to pump rotors that have a normalized specific speed of less than 0.8. This region applies primarily to centrifugal pumps.

$$\eta_{\text{hyd,design}} = 0.41989 + 2.1524 \, Ns - 3.1434 \, Ns^2 + 1.5673 \, Ns^3 \tag{24}$$

Pump rotors that have design-point specific speeds above 0.8 are primarily of the mixed-flow and axial (or inducer) type, and are represented by equation (25). There can be extensive overlap in the design-point specific speed range between axial, mixed-flow, and centrifugal configurations. The efficiency correlation assumes that an appropriate pump configuration has been selected and optimized by the designer for a given application.

7

$$\eta_{\text{hyd,design}} = 1.020 - 0.120\,Ns \tag{25}$$

The total pressure of the rotor exit is estimated from the rotor head rise with equation (26). Here the fluid density is averaged to allow for small variations through the rotor. This is done primarily in the case of liquid hydrogen which is slightly compressible.

$$P_{t2} = \frac{H_2\,\rho_{\text{avg}}}{144} + P_{t1} \tag{26}$$

The static pressure is calculated from the local velocity and the total pressure with

$$P_s = P_t - \frac{C^2\,\rho}{2 \times 144\,g_c} \tag{27}$$

Off-Design Rotor Efficiency

Once the design point rotor efficiency is determined by the specific speed relation, it is varied at off-design operating conditions. The hydraulic efficiency variation at off-design is due to additional friction and incidence losses. The flow-speed ratio compared to the design flow-speed ratio is defined by the parameter shown in the following equation:

$$F = \frac{(Q/N)}{(Q/N)_{\text{design}}} \tag{28}$$

The off-design variation of rotor efficiency has been empirically derived from pump data (ref. 4) for values of F between 0.7 and 1.2 while the extremities of the curve were extrapolated from present data. A plot showing the efficiency variation is shown in figure 5 and is expressed by equation (29) in terms of F and the design point rotor efficiency.
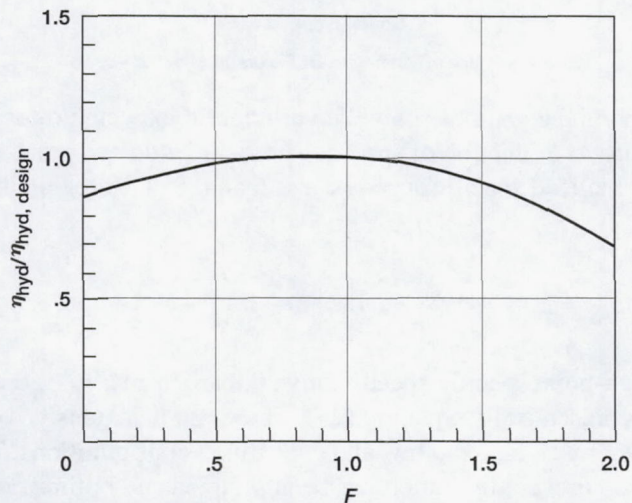

Figure 5.—Rotor efficiency at off-design flow-speed parameter.

8

$$\frac{\eta_{\text{hyd}}}{\eta_{\text{hyd,design}}} = 0.86387 + 0.3096\,F - 0.14086\,F^2 - 0.029265\,F^3 \tag{29}$$

Suction Performance

Although the code models only noncavitating pump performance, it can estimate whether cavitation is likely to occur based on empirical correlations and assumptions on blade-to-blade loading. Since PUMPA is a meanline method, it can only model flow conditions in the meridional plane and does not model the details of the flow within the blading. However, assumptions can be made that permit an estimate of the flow conditions within the blade by multiplying the inlet velocity with a user-specified blade-to-blade loading parameter (*BB*). The region within the blade near the tip is where the local static pressure is expected to be the lowest and where cavitation is most likely to be initiated at flow rates above the design value. The tip velocity upstream of the blade is multiplied by *BB* to estimate the velocity of the fluid on the suction side of the blade near the throat. The local static pressure at the throat is calculated from the estimated velocity there and the inlet total pressure as follows:

$$P_{s,\text{throat}} = P_{t1} - \frac{\left(C_1\,BB\right)^2 \rho_1}{2 \times 144\,g_c} \tag{30}$$

The local static pressure is compared to the local vapor pressure to check for the onset of cavitation. Values for the loading parameter can be in the range of 1.1 to 1.3 at the design speed and flow condition. A value of 1.2 for *BB* can estimate the onset of cavitation to within 10 percent. A more accurate estimate of the loading parameter can be determined by flow codes of higher fidelity, but is not necessary or feasible during conceptual design.

The net positive suction head of a pump is a function of the inlet total pressure and the vapor pressure of the fluid and is calculated as follows:

$$NPSH = \frac{144\,(P_{t1} - P_v)}{\rho_1} \tag{31}$$

The vapor pressure is obtained from the fluid properties package within the GASPLUS (ref. 2) code. The suction-specific speed of the pump is defined as:

$$Nss = \frac{N\,Q^{1/2}}{\left(NPSH + TSH\right)^{3/4}} \tag{32}$$

The thermodynamic suppression head (*TSH*) is calculated only for liquid hydrogen and is considered negligible for the other fluid options. *TSH* has been empirically derived for liquid hydrogen as a function of temperature and is represented by the following:

$$TSH = 0.415\,(T_t - 20.0)^2 \tag{33}$$

The suction performance capability at off-design operating conditions is typically lower than at the design condition. The reduced capability at off-design is normalized in the code by the flow-speed ratio *F*

9

of equation (28) and the design point suction-specific speed capability. The difference between the suction capability at design and at off-design can be partially attributed to flow separations due to incidence and backflow-induced inlet swirl (ref. 7) At low flow conditions, the inlet swirl caused by backflow reduces the inlet static pressure and the suction-specific speed capability. Cavitation at values of F below 1.0 can have an influence on the location of the stall line. However, more research needs to be done to quantify the correlation between cavitation and pump stall. At high flow conditions, the incidence results in flow separations and reduced flow area, also reducing the static pressure and suction-specific-speed capability as described in reference 7. Off-design suction performance is estimated with the normalized suction-specific speed curve shown in figure 6 that is referenced to the design point suction capability. The normalized curve is empirically derived from several tested pump configurations. The normalized curve at off-design is represented in the PUMPA code by the polynomial shown below:

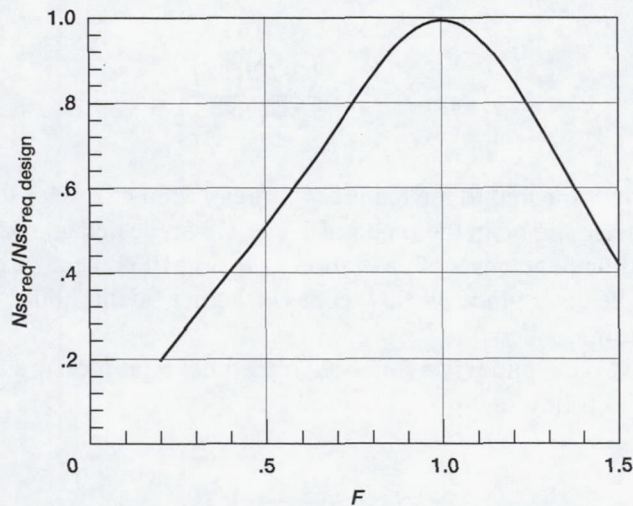$$Nss_{req} = -0.28607 + 4.14245\,F - 12.0967\,F^2 + 20.708\,F^3 - 15.42122\,F^4 + 3.9366\,F^5 \tag{34}$$

Figure 6.—Suction performance at off-design flow-speed parameter.

Off-Design Rotor Head

As at design condition, the rotor Euler head rise at off-design operating conditions is also calculated from the velocity triangles. An additional factor is applied at off-design in order to compensate for effects such as impeller backflow and changes in slip and boundary layer blockages from their design values. The empirically derived factor compensates for additional rotor head rise due to these effects, which are not otherwise modeled in this meanline code. To compensate for these effects, the factor is applied to the design-point slip σ. This additional correction factor is shown in the curve of figure 7 as a function of flow-speed parameter F, which is represented in PUMPA by the polynomial

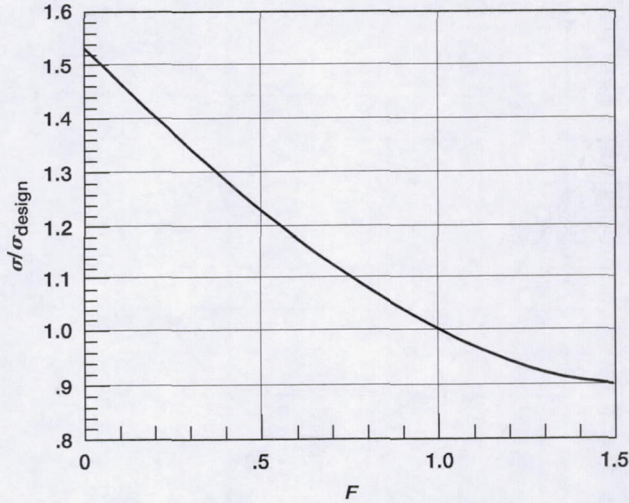$$\frac{\sigma}{\sigma_{design}} = 1.534988 - 0.6681668\,F + 0.077472\,F^2 + 0.0571508\,F^3 \tag{35}$$

10

Figure 7.—Slip factor at off-design flow-speed parameter.

Diffusion System Pressure Recovery and Loss

The total pressure loss coefficient of the diffusion system design point is assumed to be known and is input in terms of a normalized loss coefficient. The loss coefficient is expressed in terms of normalized parameters at the rotor exit and the total pressure loss through the diffusion system in the following equation:

$$\omega_{2-4} = \frac{P_{t2} - P_{t4}}{P_{t2} - P_{s2}} \tag{36}$$

The minimum loss coefficient (typically near the design point) can vary between 0.15 to 0.25 for pumps having vaneless diffusers followed by volutes, provided that the rotor and the volute are properly matched. The fluid velocity at the throat of the vaned-diffuser volute or is calculated by the relation shown here:

$$C_{\text{throat}} = \frac{144\, m}{\rho\, A_{\text{throat}}} \tag{37}$$

The loading parameter is defined in terms of the velocities at the vaneless diffuser exit and the velocity at the diffusion system throat:

$$L = \frac{C_{\text{throat}}}{\left(C_{U3}{}^2 + C_{M3}{}^2\right)^{1/2}} \tag{38}$$

The normalized pressure loss coefficient of the diffusion system, as a function of the loading parameter, is shown in figure 8 and is used for vaneless-diffuser-volute, vaned-diffuser-volute, and crossover, configurations.

The empirically derived variation of total pressure loss coefficient as a function of loading is described by the following polynomial:

$$\frac{\omega_{2-4}}{\omega_{2-4,\text{design}}} = 1.8151 - 1.83527\, L + 0.8798\, L^2 + 0.18765\, L^3 \tag{39}$$
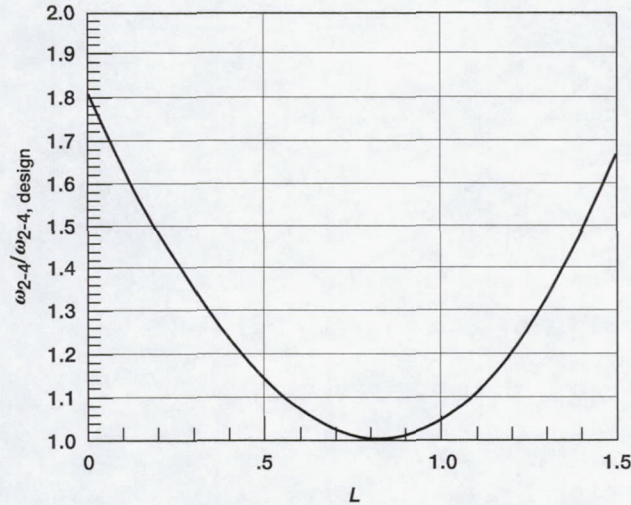
11

Figure 8.—Diffusion system pressure loss coefficient versus loading.

A key aspect of the conceptual design of the pump is sizing the diffusion system dimensions. One of the key dimensions that affects the performance of the diffusion system is the effective flow area at the throat (minimum area region). Empirical correlations to the values of diffusion system loading parameter that result in acceptable operating range have been found to be near 0.80. The value of the diffusion system loading parameter at the design point is one of the key factors that influences the shape, or slope, of the overall pump characteristic map. A pump with a high-diffusion-system loading parameter at the design operating condition will have a steep-slope characteristic performance map and may have im-proved throttling range. Pumps having a low loading parameter within the diffusion system at the design operating condition will exhibit shallower slope characteristic maps and may experience earlier stall in comparison to pumps having a high loading parameter. The location of the stall line is estimated from the empirical limit of 0.70 on the static pressure recovery coefficient of the vaneless diffuser. However, it is likely that cavitation at low flows also has an effect on pump stall (ref. 7). More work is needed to quantify the relationship of cavitation and pump stall. The diffuser stall line is obtained by post-process-ing the output.

The static pressure recovery of the diffusion system is derived from the diffusion-loss coefficient. The static pressure at the pump stage exit is calculated from local values of total pressure and velocity with

$$P_{s4} = P_{t4} - \frac{C_4^2 \rho_4}{2g_c} \tag{40}$$

where the exit velocity is determined by the mass flow rate and the exit area in the following equation:

$$C_4 = \frac{144\,m}{\rho_4 A_4} \tag{41}$$

The static pressure recovery coefficient of the diffusion system is calculated in terms of the rotor exit and stage exit conditions as follows:

$$c_{p(2-4)} = \frac{P_{s4} - P_{s2}}{P_{t2} - P_{s2}} \tag{42}$$

12

Stage Head and Power

The head rise through the pump stage is calculated from the total pressure at the stage exit by:

$$H_4 = \frac{\left(P_{t4} - P_{t1}\right)144}{\rho_{avg}} \tag{43}$$

where the value of ρ is equal to the average density of the fluid from the stage inlet (station 1) to the stage discharge (station 4). Density variations are usually negligible for all pumped fluids except liquid hydrogen.

The disk pumping (windage) loss is calculated with equation (44) by using an experimental loss (ref. 4) factor K.

$$HPd = 32\, K\, N^3\, R_{hub2}{}^5 \tag{44}$$

Volumetric efficiency is based on internal leakages and is expressed as the ratio of leakage to the inlet flow

$$\eta_{vol} = \frac{m}{m + m_L} \tag{45}$$

A default value of 98 percent mechanical efficiency due to bearing friction is used in the flow code. The stage horsepower (HP) required to drive the pump is calculated from the head rise through the rotor; the rotor hydraulic, mechanical, and volumetric efficiencies; and the disk pumping losses, as shown here:

$$HP = \frac{m\, H_2}{550\left(\eta_{hyd}\, \eta_{mech}\, \eta_{vol}\right)} + HPd \tag{46}$$

Overall pump efficiency is calculated with:

$$\eta_4 = \frac{m\, H_4}{550\, HP} \tag{47}$$

In a pump with multistages in series, the inlet conditions of the next stage are determined from the exit conditions of the previous stage. The PUMPA code stacks the performance of multistages together and provides a summary of the overall pump conditions of exit pressure, head, horsepower, and efficiency.

EXAMPLES OF PUMP ANALYSES

Several pumps (figs. 9 to 12) have been analyzed with the PUMPA flow modeling code in order to validate the normalized performance parameters within the code. The selected pumps vary in size, configuration, stage number, and pumped fluid. A cross-section view of each pump is included to illustrate the variety of configurations that have been analyzed. Pump overall performance maps were plotted from the output files generated by the PUMPA code. Test data is superimposed onto the maps created with the PUMPA flow model. Each of the sample pumps analyzed required a modification of the default values for rotor efficiency, slip factor, and diffusion system loss parameter in order to more closely match the tested exit pressure and power data. These corrections to the default values of rotor efficiency and slip factor, and the diffusion system loss coefficient, are summarized in table I.
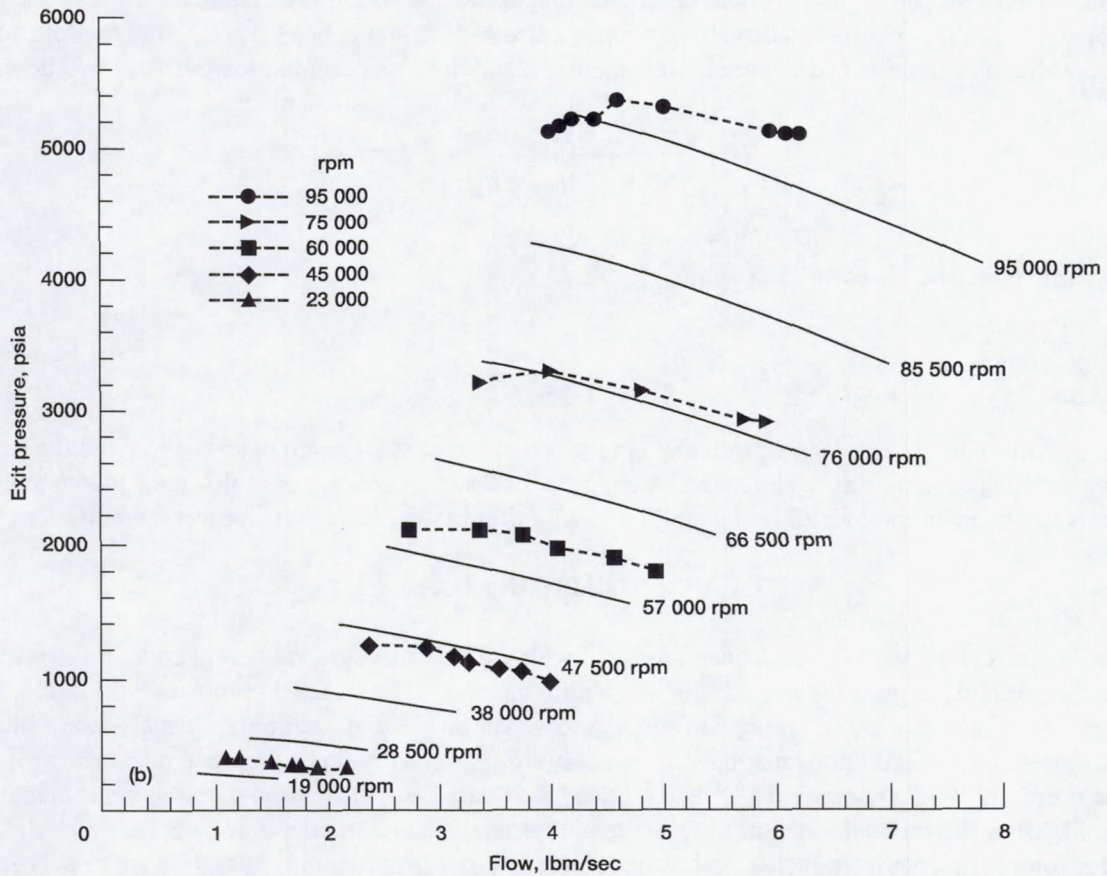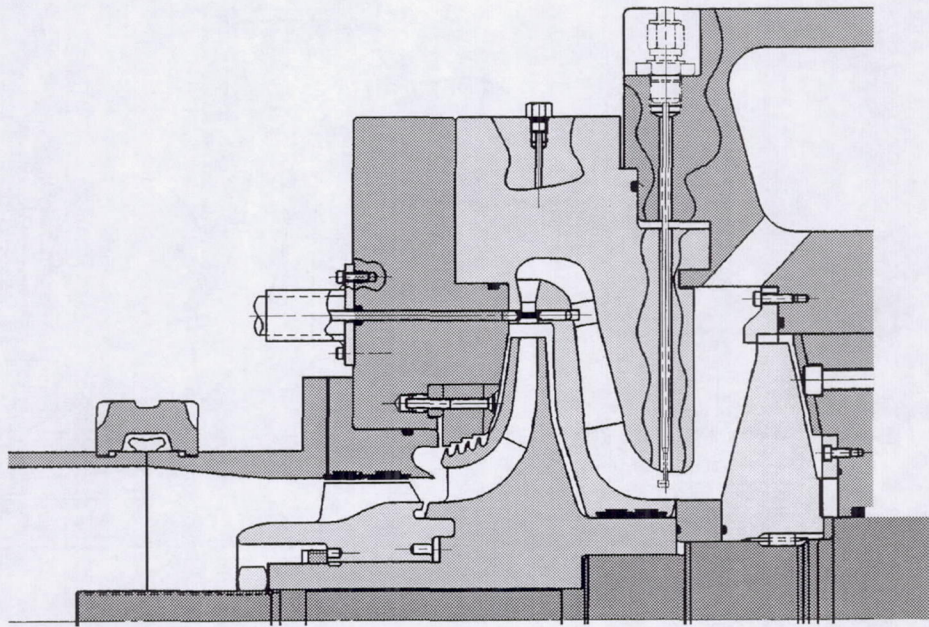
13

(a)

(b)
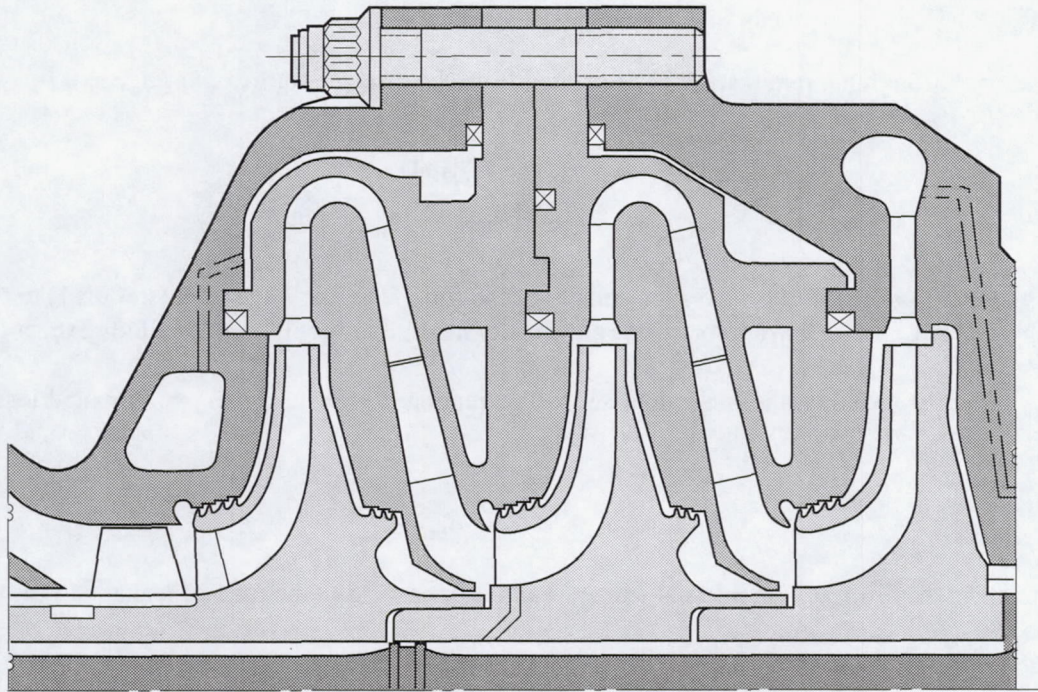
Figure 9.—MARK 48 liquid hydrogen pump. (a) Cross-section view. (b) Pump overall performance map ($P_1 = 71$; $T_1 = 38$).
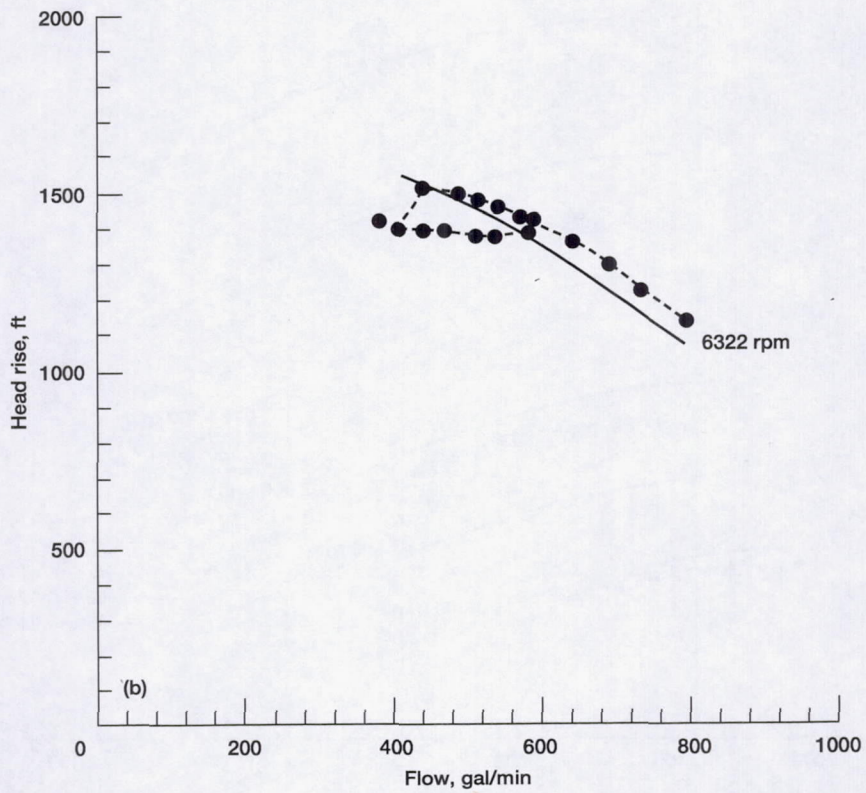
14

(a)

6322 rpm

(b)

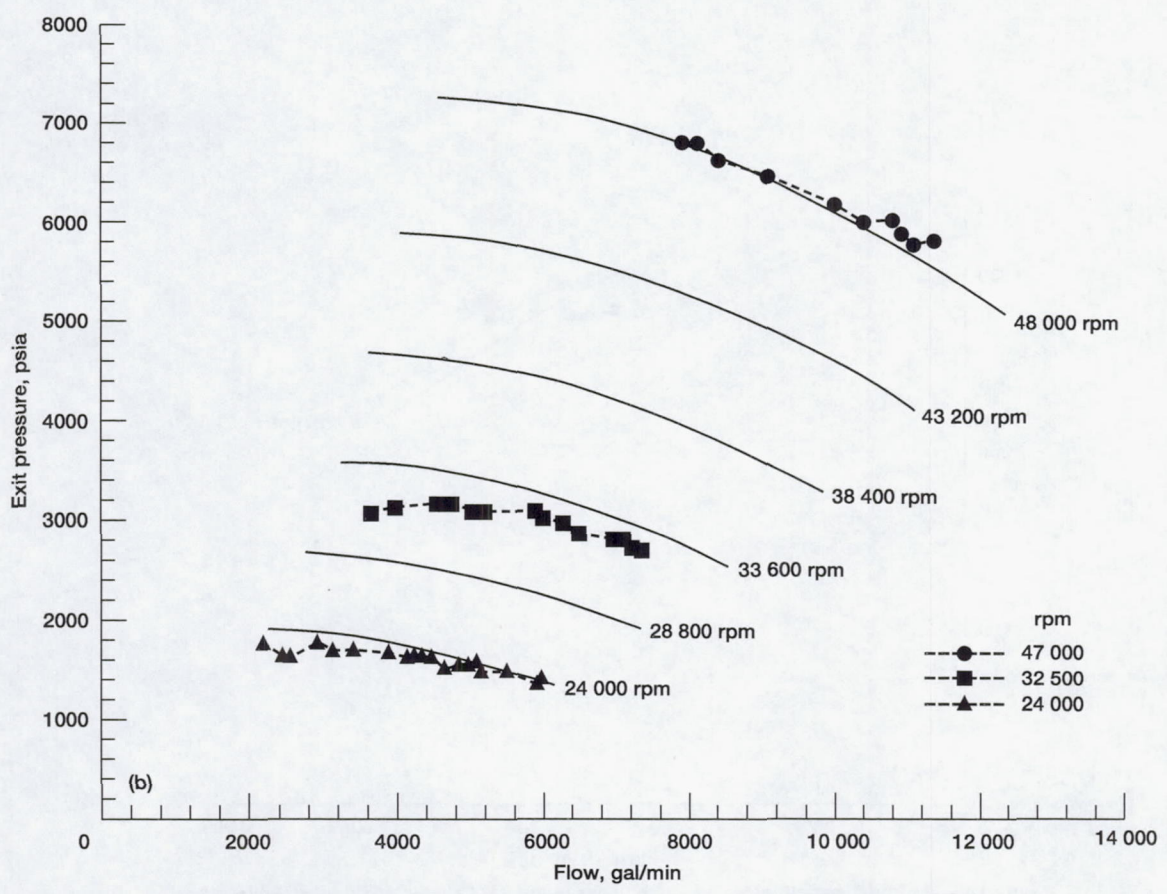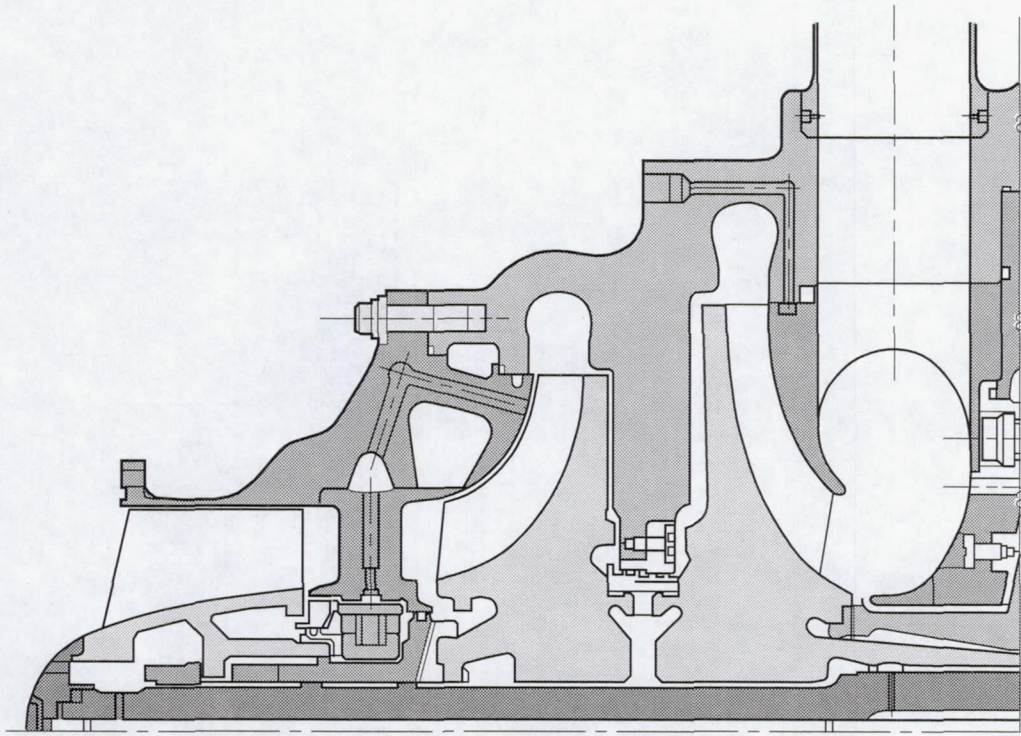Figure 10.—MARK 49 scaled tester research water pump. (a) Cross-section view. (b) Pump overall performance map.

Figure 11.—XLR-129 high pressure liquid hydrogen pump. (a) Cross-section view. (b) Pump overall performance map ($P_1 = 116.9$; $T_1 = 46.4$).
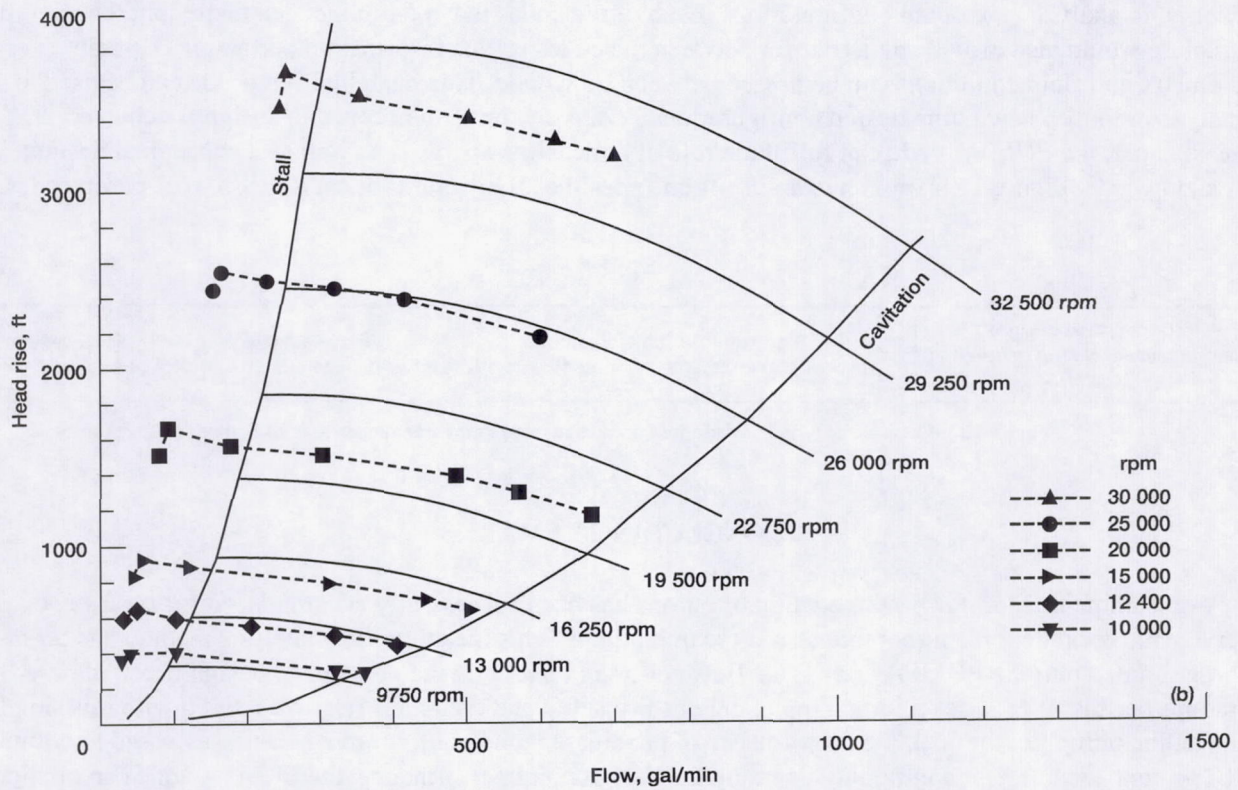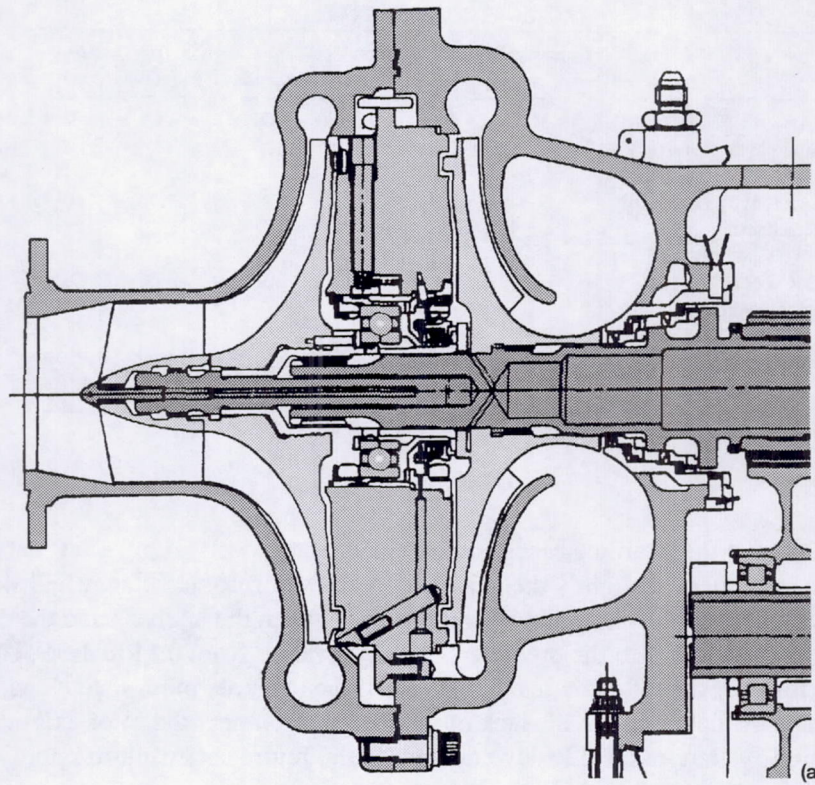
Figure 12.—RL10A-3-3A liquid hydrogen pump. (a) Cross-section view. (b) Pump overall performance map (P_1 = 28; T_1 = 38).

TABLE I.—CORRECTIONS TO THE DEFAULT VALUES AND DIFFUSION SYSTEM
LOSS COEFFICIENT

Pump	Figure	Reference	Configuration	η_{hyd} correction	σ correction	ω_{2-4}
MARK 48 liquid hydrogen	9	8	1 Inducer 3 Centrifugals	1.06	1.02	0.19
MARK 49 H_2O scaled tester	10	9	1 Inducer 1 Centrifugal	0.81	1.00	0.23
XLR–129 HP liquid hydrogen	11	10	1 Inducer 2 Centrifugals	1.02	1.00	0.21
RL10A–3–3A liquid hydrogen	12	11	1 Inducer 2 Centrifugals	0.97	1.00	0.20

DISCUSSION

The meanline analyses of the example cases compare reasonably well with the test data. As shown in table I, it was necessary to modify slightly the calculated values of rotor efficiency and slip factor by means of a correction factor in order to improve the match between the analysis and the data. For the cases studied, the correction factor to the predicted rotor loss varied from 0.81 to 1.06. The predicted slip factor was corrected for only one of the cases. For many of the example pumps analyzed, only the overall head-flow-speed data is available due to the lack of instrumentation near the rotor exit to determine rotor efficiency and diffusion system loss. Code development in the future can result in improvements that may reduce the need for the correction factors listed in table I.

PUMPA can be used as part of a system of flow codes, each with a specific purpose and level of fidelity, to analyze new pump configurations. Each of the codes may be run independently, but the overall structure would also provide data transfer between the codes so that information pertaining to pump geometry and fluid conditions can be passed between each code. This meanline flow code can be used to analyze proposed new pump design configurations iteratively, until an acceptable design is achieved. In this manner, the PUMPA code can fulfill the role of a meanline analysis, as well as a conceptual design, or sizing code. Figure 13 shows an example of one possible architecture for such a system of pump codes.
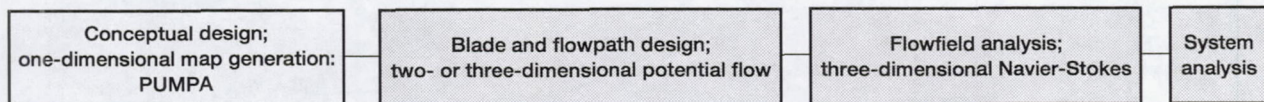

Figure 13.—Example of types of code functionalities used in the design process of pumps.

CONCLUDING REMARKS

A meanline method for flow modeling of pumps has been successfully accomplished for a variety of cryogenic rocket engine turbopumps and research pumps. This meanline flow analysis method has been programmed into the PUMPA code. This flow code can be used in the conceptual design phase of new pumps because it requires minimal input and has fast setup and computer run times. Even with this simple meanline pump flow model, the performance of candidate pump configurations can be assessed to within 10 percent accuracy. In addition to assessing the design point performance, the PUMPA code can predict the shape of the pump off-design head-flow characteristic performance map and can provide pump maps for system evaluation of the complete rocket engine.

APPENDIX—SYMBOLS

A area, in.^{2}

B blade span from hub to tip, in.

BB blade-to-blade loading parameter at blade throat

Bk blade metal blockage, in.^{2}

C absolute fluid velocity, ft/sec

c_p static pressure recovery coefficient of diffusion system

F flow-speed ratio compared to the design condition

g_c gravitational constant, 32.174 lbm-ft/lbf-sec^2

HP power transmitted to pumped fluid, hp

HPd power lost due to disk pumping

H head rise, ft

i incidence between fluid relative flow angle and blade angle at inlet, deg

K disk pumping loss factor

L loading parameter

m mass flow, lb/sec

$NPSH$ net positive suction head, ft

N shaft rotative speed, r/min

Ns specific speed

Nss suction-specific speed

P pressure, psia

Q flow, gal/min

R radial distance from pump centerline, in.

S blade length from inlet to exit midspan, in.

slip   difference between the theoretical and absolute fluid tangential velocities

19

T	temperature, °R
Thk	normal blade thickness, in.
TSH	thermodynamic suppression head, ft
U	blade tangential velocity, ft/sec
W	relative fluid velocity, ft/sec
X	normalized blade length, $X = S + (2\,R_{\text{rms }2})$
Z	blade number including splitters or part blades
α	absolute fluid angle, degrees from tangential
β	relative angle, degrees from tangential
δ	radius ratio of rotor inlet to exit, $\delta = R_{\text{rms }1} + R_{\text{rms }2}$
η	efficiency, total-to-total
λ	boundary layer blockage factor, effective flow area / total area
ρ	fluid density, lb/ft^3
σ	Pfleiderer slip factor
ω	total pressure loss coefficient of diffusion system

Subscripts

1	rotor inlet (leading edge)
2	rotor exit (trailing edge)
3	vaneless diffuser exit
4	stage exit
avg	average
B	blade
design	condition at design flow and speed
F	fluid
hub	hub region of flowpath

hyd	hydraulic
i	ideal
L	leakage mass flow
M	meridional component, $C_M^2 = C_x^2 + C_r^2$
mech	mechanical loss due to friction
r	radial component
req	required, or allowable (Nss)
rms	root-mean-square
s	static
t	total (stagnation)
TH	theoretical
throat	minimum area region of rotor or diffusion system
tip	tip region of flowpath
U	tangential component of velocity
v	vapor
vol	volumetric loss due to leakage
x	axial component

REFERENCES

1. Hannum, N.P.; Berkopec, F.D.; and Zurawski, R.L.: NASA's Chemical Transfer Propulsion Program for Pathfinder. NASA TM–102298, 1989 (Also, AIAA Paper 89–2298, 1989).

2. Fowler, J.R.: GASPLUS User's Manual. NASP CR–1012, Mar., 1988.

3. Kovats, A.: Design and Performance of Centrifugal and Axial Flow Pumps and Compressors. Macmillan, New York, 1964.

4. Stepanoff, A.J.: Centrifugal and Axial Flow Pumps: Theory, Design, and Applications. Wiley, New York, 1957

5. Pfleiderer, C.: Turbomachines. Springer-Verlag, New York, 1952.

6. Rodgers, C.: Efficiency of Centrifugal Compressor Impellers. Centrifugal Compressors, Flow Phenomena, and Performance, AGARD CP–282, Paper 22, 55th (B) Specialists Meeting of the Propulsion and Energetics Panel of AGARD, Brussels, Belgium, 1980.

7. Veres, J.P.: A Survey of Instabilities Within Centrifugal Pumps and Concepts for Improving the Flow Range of Pumps in Rocket Engines. 1992 JANNAF Propulsion Meeting, Vol. 1, D.S. Eggleston, ed., CPIA–PUBL–580–VOL–1, 1992, pp. 615–629 (Also, NASA TM–105439, 1992).

8. Csomor, A.; and Warren, D.J.: Small, High-Pressure Liquid Hydrogen Turbopump. NASA CR–159821, 1980.

9. Larivier, B.: Orbital Transfer Rocket Engine Technology, High Velocity Ratio Diffusing Crossover. NASA Contract No. NAS3–23773 Task B.2, Rockwell Intl, Rocketdyne Div., Dec. 1992.

10. Atherton, R.R.: Air Force Reusable Rocket Engine Program XLR-129-P-1, Demonstrator Engine Design. Report AFRPL–TR–70–6, Pratt & Whitney, Air Force Rocket Propulsion Laboratory, Air Force Systems Command, Edwards Air Force Base, Apr. 1970.

11. Wanhainen, A.; and Hannum, M.: Throttling Characteristics of a Hydrogen-Oxygen, Regeneratively Cooled, Pump-Fed Rocket Engine. NASA TM X–1043, 1964.

REPORT DOCUMENTATION PAGE

Form Approved
OMB No. 0704-0188

1. AGENCY USE ONLY (Leave blank)	2. REPORT DATE	3. REPORT TYPE AND DATES COVERED
	February 1995	Technical Memorandum

4. TITLE AND SUBTITLE

Centrifugal and Axial Pump Design and Off-Design Performance Prediction

5. FUNDING NUMBERS

WU–505–62–5J

6. AUTHOR(S)

Joseph P. Veres

7. PERFORMING ORGANIZATION NAME(S) AND ADDRESS(ES)

National Aeronautics and Space Administration
Lewis Research Center
Cleveland, Ohio 44135–3191

8. PERFORMING ORGANIZATION REPORT NUMBER

E–9157

9. SPONSORING/MONITORING AGENCY NAME(S) AND ADDRESS(ES)

National Aeronautics and Space Administration
Washington, D.C. 20546–0001

10. SPONSORING/MONITORING AGENCY REPORT NUMBER

NASA TM–106745

11. SUPPLEMENTARY NOTES

12a. DISTRIBUTION/AVAILABILITY STATEMENT

Unclassified - Unlimited
Subject Category 20

12b. DISTRIBUTION CODE

13. ABSTRACT (Maximum 200 words)

A meanline pump-flow modeling method has been developed to provide a fast capability for modeling pumps of cryogenic rocket engines. Based on this method, a meanline pump-flow code PUMPA was written that can predict the performance of pumps at off-design operating conditions, given the loss of the diffusion system at the design point. The design-point rotor efficiency and slip factor are obtained from empirical correlations to rotor-specific speed and geometry. The pump code can model axial, inducer, mixed-flow, and centrifugal pumps and can model multistage pumps in series. The rapid input setup and computer run time for this meanline pump flow code make it an effective analysis and conceptual design tool. The map-generation capabilities of the code provide the information needed for interfacing with a rocket engine system modeling code. The off-design and multistage modeling capabilities of PUMPA permit the user to do parametric design space exploration of candidate pump configurations and to provide head-flow maps for engine system evaluation.

14. SUBJECT TERMS

Centrifugal; Axial; Pump; Performance; Design; Off-design; Meanline; Flow; Model; Rocket; Turbopump

15. NUMBER OF PAGES
24

16. PRICE CODE
A03

17. SECURITY CLASSIFICATION OF REPORT	18. SECURITY CLASSIFICATION OF THIS PAGE	19. SECURITY CLASSIFICATION OF ABSTRACT	20. LIMITATION OF ABSTRACT
Unclassified	Unclassified	Unclassified	

NSN 7540-01-280-5500

Standard Form 298 (Rev. 2-89)
Prescribed by ANSI Std. Z39-18
298-102